Federico Gulisano[a*], Thanyarat Buasiri[b], Freddy Richard Apaza Apaza[a], Andrzej Cwirzen[b], Juan Gallego[a]

[a] Departamento de Ingeniería del Transporte, Territorio y Urbanismo, Universidad Politécnica de Madrid, C/Profesor Aranguren 3, 28040 Madrid, Spain

[b]Building Materials, Department of Civil, Environmental and Natural Resources Engineering, Luleå University of Technology, 97187 Luleå, Sweden

Piezoresistive behaviour of electric arc furnace slag and graphene nanoplatelets asphalt mixtures for self-sensing pavements

Abstract

Self-sensing road pavements can autonomously monitor their stress/strain and damage states without the need for embedded sensors. This kind of multifunctional pavements could be used for the realisation of autonomous structural health monitoring (SHM) systems. Moreover, it would permit to collect important traffic data for traffic-monitoring analysis and the development of Vehicle to Infrastructure Communication (V2I) tools, hence contributing to the digitalisation of the transport sector. The sensing mechanism is based on the piezoresistive effect, consisting of a change in the electrical response of the road material when subjected to stress/strain or damage. This paper aims to investigate the piezoresistive behaviour of conductive asphalt mixtures with electric arc furnace slag (EAFS) and graphene nanoplatelets (GNPs) for self-sensing application. The results showed that asphalt mixtures with EAFS as fine aggregate and 7 wt% of GNPs exhibited excellent self-sensing properties for both traffic monitoring and SHM systems.

1. Introduction

Multifunctional pavements not only guarantee the traditional functions of road pavements (e.g., resisting traffic loads and providing a safe and comfortable surface) but also possess additional non-structural functions, to face the new challenges of EU agreements toward the decarbonization and digitalization of the road transport sector. Examples of multifunctional pavements are those that charge Electric Vehicles (EVs) while they are in motion [1], harvest energy from the traffic loading [2], and self-heal their cracks [3,4].

Self-sensing pavements are another example of multifunctional pavements, which can autonomously monitor their stress/strain and damage states, continuously and in real-time.

Self-sensing properties are achieved by designing the road pavement with partially conductive asphalt mixture. Self-sensing mechanism is based on the piezoresistive effect. As the conductive asphalt mixture is stressed or damaged under the effect of traffic loads, the geometry of the internal conductive network slightly changes, affecting the ultimate electrical resistance of the material. This enables the detection of the material's stress/strain or damage states by measuring the pavement's electrical response. The ability of the material to response to the external stimuli by changing its electrical properties is an indicator of self-sensing properties [5].

In contrast with the use of embedded or attached sensors, such as piezoelectric sensors [6] or optical fibres [7], self-sensing asphalt materials are themselves sensors, thus performing both structural and sensing functions. Compared with other sensors, the main advantages of self-sensing materials are the low cost, high sensitivity, excellent compatibility, high durability, mechanical strength, and low maintenance cost [8,9].

In the field of road infrastructures, self-sensing pavements can be used to monitor the internal structural conditions of the road pavements.

Self-sensing pavements are expected to be mainly used for monitoring the cracking phenomenon in asphalt pavements. It was observed that the formation and propagation of cracks disturb the conductive network inside the mixture, increasing the electrical resistance [10].

Rutting phenomenon could also be monitored with these kinds of pavements. The accumulation of plastic deformations due to the viscoelastic nature of asphalt mixtures can produce changes in the electrical response. Although some studies were performed [8,11], further research is necessary to find a clear relationship between rutting and the electrical response of asphalt materials.

Together with other innovative technologies aimed at detecting surface cracks [12] and texture properties [13] with computer-vision and machine learning algorithms, these kinds of pavements would contribute to the development of automatic structural health monitoring (SHM) systems. Furthermore, such systems allow the possibility of planning maintenance operations based on continuous monitoring of the structural condition of the pavement to feed prediction models supported by artificial intelligence (i.e., predictive maintenance) rather than on a fixed schedule, enhancing the efficiency of the budget-allocation strategy [14].

Self-sensing pavements can also be used for collecting important traffic data, such as flow, speed, and weight of vehicles [15–17]. These data can be helpful in traffic-monitoring analysis and weigh-in-motion applications. Moreover, the collected traffic data can also be shared with road users by developing Vehicle to Infrastructure Communication (V2I) tools based on self-sensing pavements, hence contributing to the digitalization of the transport sector.

The working principle of the self-sensing pavement is described in Fig. 1. Some electrodes are included in the road pavement and connected with an external multimeter to collect the electrical data. The electrical data, which permits estimating the pavement's stress/strain or damage state, are then sent to the data center for its analysis by using a transmitting antenna. SHM and traffic monitoring systems are then developed based on the collected data.

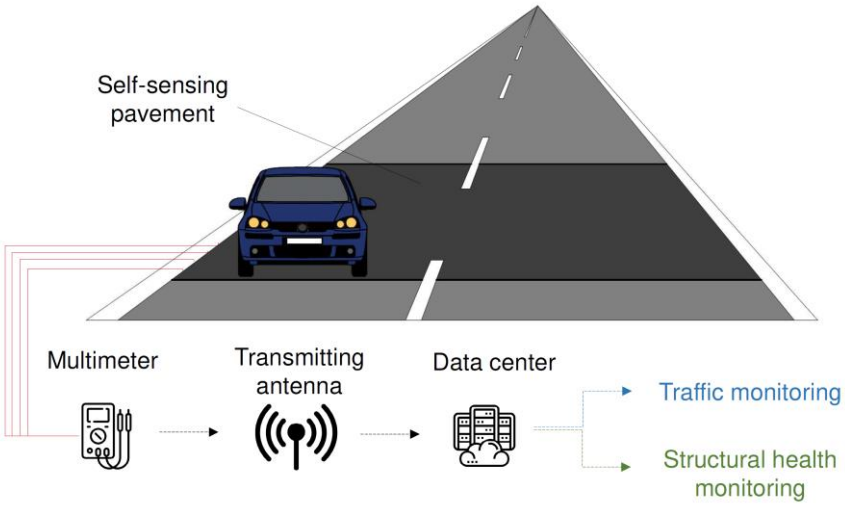

Fig. 1. Working principle of self-sensing pavement

The self-sensing mechanism of cement-based materials has been extensively investigated [9,18–20], and the feasibility of this technology at full-scale in concrete road pavements [15,16]. However, literature on the self-sensing performance of asphalt-based materials is very limited, and there is undoubtedly an urgent need for further research on this topic.

Although conventional asphalt mixture is an insulator [21], it is theoretically feasible to enhance the conductivity of asphalt pavement by adding conductive additives [22]. This is mainly due to two kinds of conductive mechanisms [20], a) contacting conduction, due to the direct contact of conductive particles, thus forming conductive paths, and b) tunneling effect, a quantum-mechanical effect that takes place when the disconnected particles are close enough to allow the transport of electrons [23].

The most widely used additive in conductive asphalt mixtures are typically carbon-based and metallic-based materials, such as carbon fibres (CF) [22,24,25], graphite [22,24–27], carbon black [22], graphene [28], carbon nanotubes [29], steel slag [21,28,30] and steel fibres [26,27]. Although the addition of conductive additives in asphalt mixtures showed their effectiveness in several applications [31,32], like road deicing [33] or induction healing [34], research on the piezoresistive response of conductive asphalt mixtures is very limited.

Piezoresisitivity effect consists in the change in the electrical resistance of a material when subjected to strain/stress and is typically described by the fractional change in resistance (FRC), in %, given by:

$$FCR\ (\%) = \frac{R - R_0}{R_0} \cdot 100 = \frac{\Delta R}{R_0} \cdot 100 \quad (1)$$

Where R_0 is the initial electrical resistance, and R is the current electrical resistance. FCR gives a measurement of the sensing properties of the material. For a fixed change in the stress/strain state, the more sensitive material is those with higher FCR.

The capability of the conductive asphalt mixture to detect the traffic flow is typically evaluated with a repeated cyclic loading test aimed at simulating the traffic loads and assessing the piezoresistive response. Conductive asphalt mixtures exhibited excellent sensing response under compression sinusoidal, creep, and haversine cyclic loading [11,24,35]. However, other authors observed a decrease in the piezoresistive response after some cycles, probably due to the deterioration of the mixture [10,24].

The variation in the electrical resistance of conductive asphalt-based materials when subjected to an external load, i.e., piezoresistive effect, is due to the combination of three effects [8], a) Proximity effect, caused by the approach or separation of conductive particles during compression and tension stress, respectively, b) Microcracks formation, which causes the cut of some conductive paths and the decrease of the resistance, and c) Dislocation of conductive paths, caused by the viscoelastic properties of asphalt mixtures, which prevent the totally recover of the original strain state after loading. The three effects coexist, and the output resistance is a combination of them. However, the factors affecting the predominance of one effect over the other are still uncertain. Some authors [11,35] obtained a positive reversible piezoresistive effect during the cyclic loading test, indicating that the resistance decreased during loading and increased during unloading, showing that the proximity effect seemed to be the predominant mechanism. However, another study observed a negative irreversible piezoresistive effect [36], indicating that the resistance increased during loading and decreased during unloading. The formation of microcracks and the dislocation of conductive paths are the predominant piezoresistive

mechanism in this case. According to previous research, the piezoresistive mechanisms of asphalt mixtures are illustrated in Fig 2.

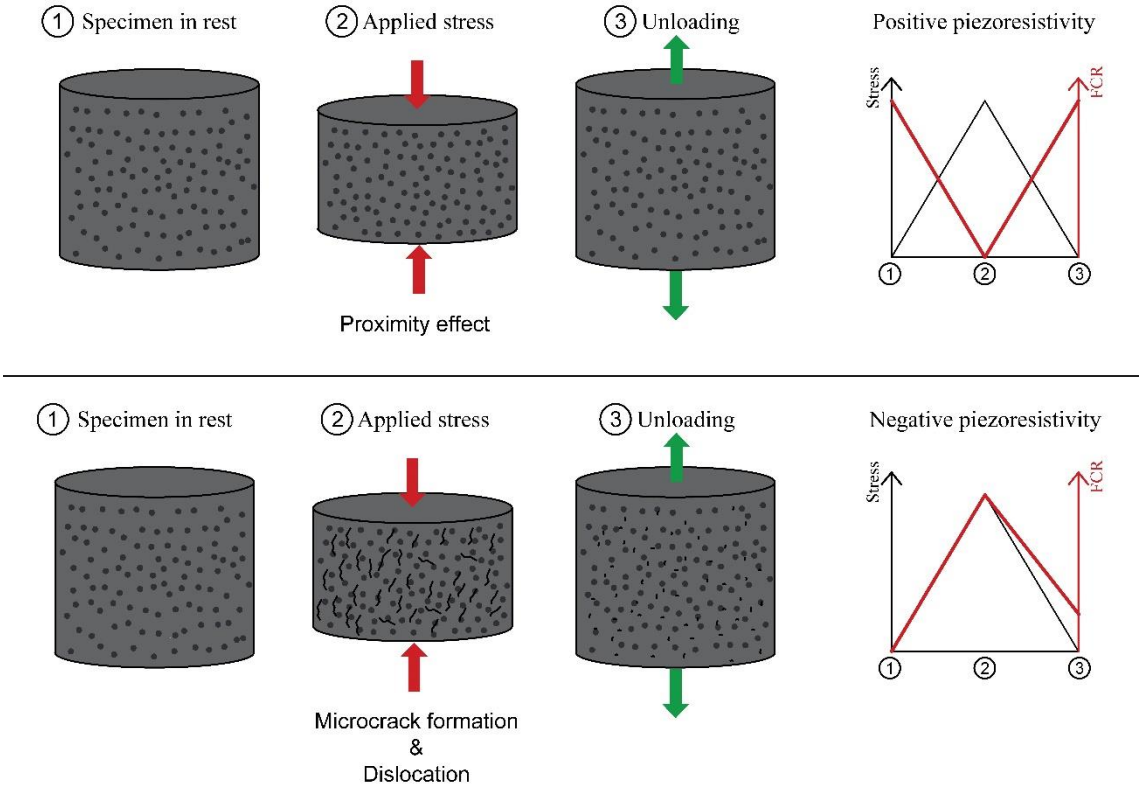

Fig. 2. Piezoresistive mechanism of conductive asphalt mixtures

To evaluate the ability of conductive asphalt mixture to sense its damage condition for SHM applications, the electrical response during destructive tests can be assessed. The working principle of a hypothetical structural health monitoring (SHM) system based on the piezoresistive effect of asphalt pavement is shown in Fig 3.

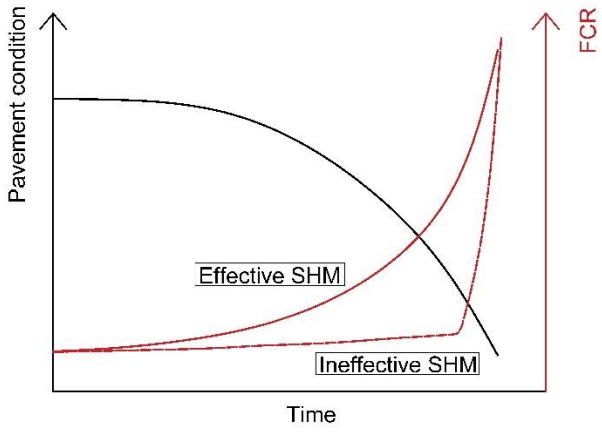

Fig. 3. SHM system based on the piezoresistive effect

It can be observed that an effective SHM system would be useful if the FCR gradually increases with the deterioration of the pavement, due to the formation of microcracks and the cut of conductive paths. In a recent study, Liu et al. [37] obtained a gradual increase in the electric resistivity with the strain during the fatigue test. However, other authors [8,10] found that the FCR remains almost stable during the fatigue test, until an abrupt increase in the resistivity before

the failure of the specimens. In this case, proper control of the deterioration state during the lifespan of the pavement would be difficult.

Despite the promising results of the studies mentioned above, further research on the piezoresistive response of asphalt mixtures is needed. The piezoresistive mechanism of conductive asphalt mixture is still uncertain. Moreover, the effect of adding electric arc furnace slag (EAFS) and graphene nanoplatelets (GNPs) on the self-sensing properties of the asphalt mixture has not been yet investigated.

The main objective of this paper is to assess the piezoresistive behavior of conductive asphalt mixtures with EAFS and GNPs for self-sensing application. A cyclic compressive test was used to evaluate the self-sensing performance of asphalt mixtures for traffic detection purposes. On the other hand, the compression test performed until failure was used to assess the performance of the mixture for SHM operations.

2. Materials

2.1. Composition of the mixtures

Stone Mastic Asphalt (SMA 11) [EN 13108-5] mixture was used in this research, which composition is shown in Table 1.

Table 1. Size distribution of the asphalt mixtures

Size (mm)	16	11.2	8	4	2	0.5	0.063
Passing (%)	100	95.3	69.7	32.3	29.4	18.8	8

Polymer-modified bitumen PMB 45/80-65 [EN 14023] was used as a binder.

In the present research, five types of asphalt mixtures were fabricated.

Reference mixture was fabricated without any additives for comparison purposes. The mixture was made with porphyry aggregate (0.063/16 mm) and calcium carbonate (CaCO3) as filler. A bitumen content of 5% by weight of the mixture was used for the Reference mixture.

EAFS mixture consisted of porphyry coarse aggregate (4/16 mm) and EAFS fine aggregate (0/4 mm). EAFS slag is a steelmaking waste; hence its use contributes to the reduction of the environmental impact of road construction. Besides improving the mechanical properties of asphalt mixtures [38], EAFS was found to be suitable for other kinds of applications, such as microwave-assisted self-healing [4,30,39]. Furthermore, its high electrical conductivity [31] makes EAFS an excellent solution for self-sensing asphalt mixtures. EAFS mixture was fabricated to evaluate the effect of adding EAFS to the asphalt mixtures. Due to the high porosity of EAFS [38], various researchers recommend increasing the bitumen content [40,41]. In the present research, to obtain volumetric properties comparable with the Reference mixture, it was chosen to use a bitumen content of 5.7% by weight of the mixture.

Other three kinds of mixtures were fabricated with EAFS as fine aggregate (0/4 mm) and GNPs at different content by weight of the bitumen: EAFS+GNPs-3%, EAFS+GNPs-5%, and EAFS+GNPs-7%. EAFS+GNPs mixtures were fabricated to enhance the electrical conductivity of the asphalt mixture and endow it with self-sensing functions. Although EAFS can enhance the electrical conductivity of asphalt mixture, bitumen, as an insulator, limits its effectiveness, acting as a barrier to the formation of conductive paths. On the contrary, GNPs directly come into contact with the bitumen, allowing the formation of conductive paths within the binder matrix. The

combined effect of both EAFS and GNPs provides the formation of an effective conductive network at the mortar level and enhances the electrical conductivity of the asphalt mixture.

The GNPs used in this research had a bulk density of 0.04 g/cm^3. The amount of layers of the GNPs was estimated to be 5-10 layers, according to the Raman Spectroscopy [42] assessed by the producer. The chemical composition of GNPs is shown in Table 2. It was essentially composed of carbon (96.41%) with traces of other elements, such as hydrogen, nitrogen, sulfur, and oxygen.

Table 2. Chemical composition of GNPs

Element	C	H	N	S	O
Percentage (%)	96.41	0.07	0.48	0.48	1.05

It was chosen to limit the addition of GNPs at 7% by weight of the bitumen, as a higher content would have compromised the workability of the mixture, according to earlier laboratory trials.

The electrical and self-sensing response was evaluated exclusively for the mixtures with GNPs, as the other mixtures (Reference and EAFS) did not show any conductive behavior.

2.2. Preparation of the specimens

The technique used in this research to measure the electrical properties of asphalt mixtures requires the embedment of four electrodes into the specimens (see Section 3). Although this is a relatively easy procedure in materials such as concrete [43], there is no consensus on the most suitable methodology for embedding electrodes in the asphalt mixture.

The method used in the present research was based on the work of Rizvi et al. [35], which found an effective technique for embedding copper wires electrodes (Fig.4) into the asphalt mixture for electrical measurements. The same authors stated that the use of copper wires, compared with copper plates, provides a smoother and better electrical signal.

Although the preparation of the specimens was performed according to the study mentioned above, some modifications were implemented.

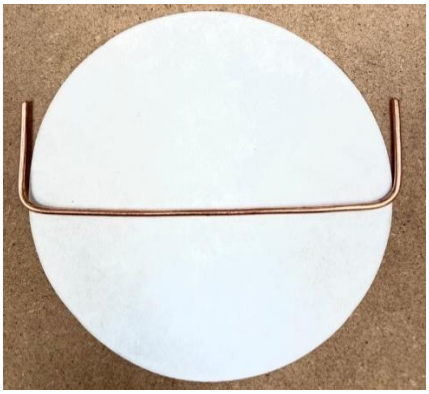

Fig. 4. Copper wire electrode

First, GNPs were incorporated into the bitumen at a temperature of 175ºC and mixed to ensure their uniform distribution. Then, aggregates and filler were added and mixed together. The loose mixture was then divided into five parts of equal mass, put into different trays, and left in an oven at 175ºC for 2h.

Later, the mixture was molded and compacted according to the procedure shown in Fig. 5. The first tray with 1/5 of the mixture was poured into the mold. Next, ten hits were applied with a piston of approximately 4 kg (Fig. 5a). This provides a first compaction of the mixture and ensures

the copper wires are positioned on a flat surface. The first copper wire was then manually placed into the mold (Fig. 5b and 5c). Next, the same procedure was applied to the following layers (Fig. 5d, 5e, 5f, 5g). Then, the mixture was compacted using a Marshall hammer [EN 12697-30:2004], applying 50 blows on each side of the specimen. Next, the specimens were left to rest for 2h and then unmolded (Fig. 5h). Finally, the copper wire ends were extracted with the help of pliers (Fig. 5i).

The final specimen (Fig. 5i) had an approximate height of 68 mm, while the four copper wires electrode had a spacing of 13.6 mm.

It should be pointed out that the above procedure was only used for assessing the electrical and piezoresistive response of asphalt mixtures. Volumetric and mechanical performance of asphalt mixtures has been determined with additional specimens fabricated with the traditional method. To evaluate the volumetric and mechanical properties of conductive asphalt mixtures, cylindrical specimens of 101 mm in diameter and approximately 68 mm in height were compacted using a Marshall hammer [EN 12697-30:2004], applying 50 blows on each side of the specimen.

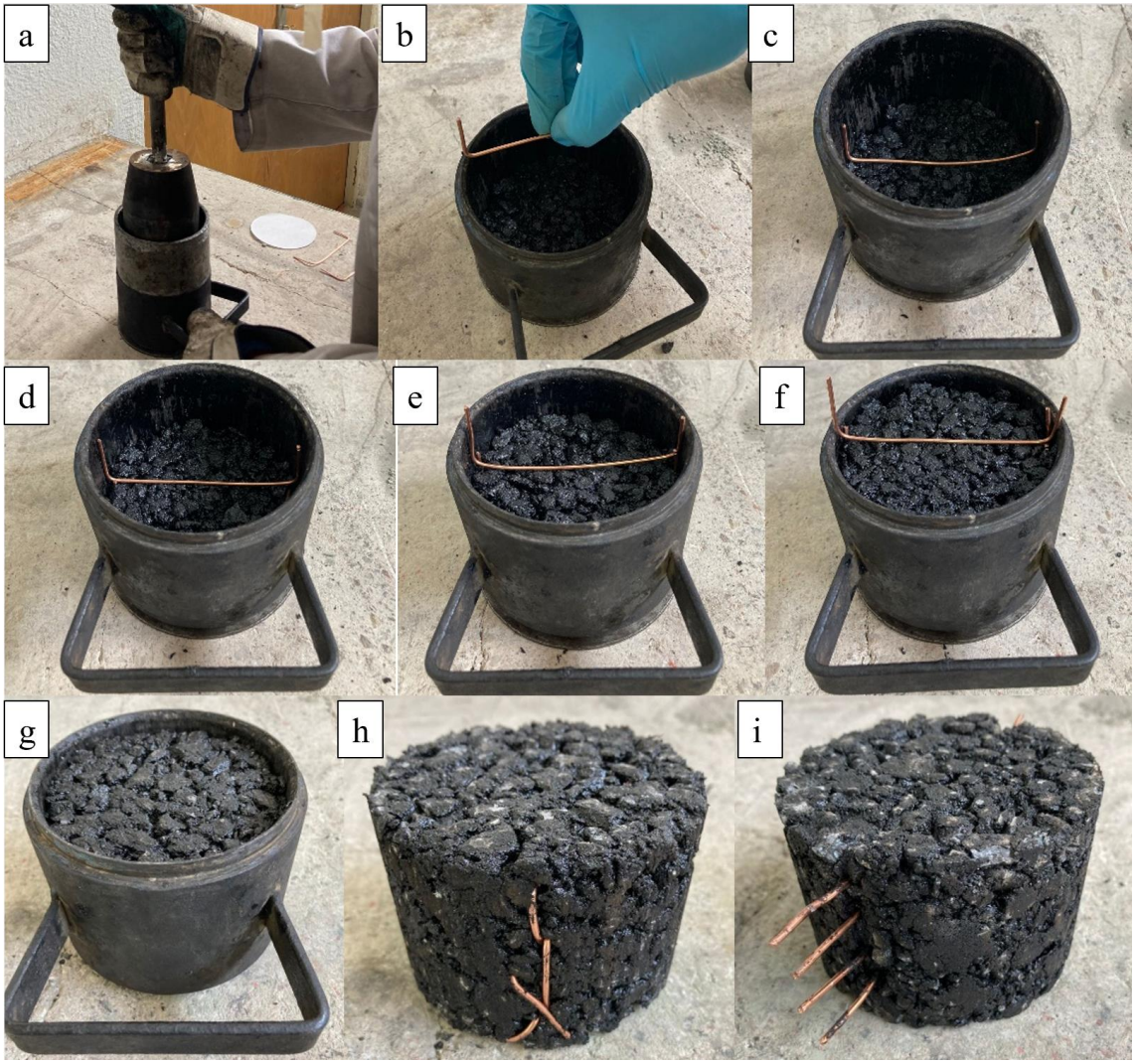

Fig. 5. Electrodes' embedment procedure

3. Experimental methodology

3.1. Volumetric and mechanical properties of conductive asphalt mixtures

The estimation of the bulk density ρ_b of asphalt mixtures was based on the saturated surface dry (SSD) method [EN 12697-6:2012]. Once obtained the bulk density and the maximum density ρ_{max} [EN 12697-5:2012], air voids content (AV) was then calculated as:

$$AV(\%) = \frac{\rho_{max} - \rho_b}{\rho_{max}} \cdot 100 \quad (2)$$

As for the mechanical characterization of the conductive asphalt mixtures, the Indirect tensile stiffness modulus (ITSM) test was conducted according to EN-12697-26:2012 standard. ITSM is defined as the relationship between applied stress and maximum measured strain response. According to the standard, five indirect tensile haversine-shaped load waveform pulses were applied with a rise time of 124 ± 4 ms to produce a target horizontal deformation of 5 ± 2 μm. The test was conducted at 20°C. ITSM, in MPa, is calculated as follows:

$$ITSM = \frac{P \cdot (\nu + 0.27)}{zh} \quad (3)$$

Where P is the maximum load (N), ν is Poisson's ratio, z is the horizontal deformation (mm), and h is the specimen thickness (mm).

Indirect tensile strength (ITS) was further assessed according to EN 12697-23:2018 standard. The test was conducted at 15°C and consisted of applying a constant deformation of 50 ± 2 mm/min until the rupture of the specimen. The Indirect tensile strength (ITS) in MPa, was calculated as:

$$ITS = \frac{2 \cdot P_{max}}{\pi \cdot d \cdot h} \quad (4)$$

Where P_{max} is the peak load, in N, d is the diameter of the specimen, in mm, and h is the height of the specimen, in mm.

3.2. Electrical measurement

The selection of the proper technique for measuring the electrical resistivity is essential for assessing the piezoresistive response of asphalt mixtures. Electrical resistivity measurement can be conducted with the two-probe or four-probe method [43]. Although most research carried out on the conductivity of asphalt mixtures using the two-probe method [10,22,24,25] due to its easier configuration, the four-probe method is recommended by many authors [18,20,44]. It allows eliminating the effects of contact resistance between electrodes and the material, thus providing more accurate measurements. For this reason, the four-probe method was used.

The asphalt specimens' electrical resistance R (Ω) was measured with a digital multimeter type Keysight 34465A. Direct current (I) was applied between the two outer electrodes, and the potential (V) was measured between the two inner electrodes [45], as represented in Fig. 6.

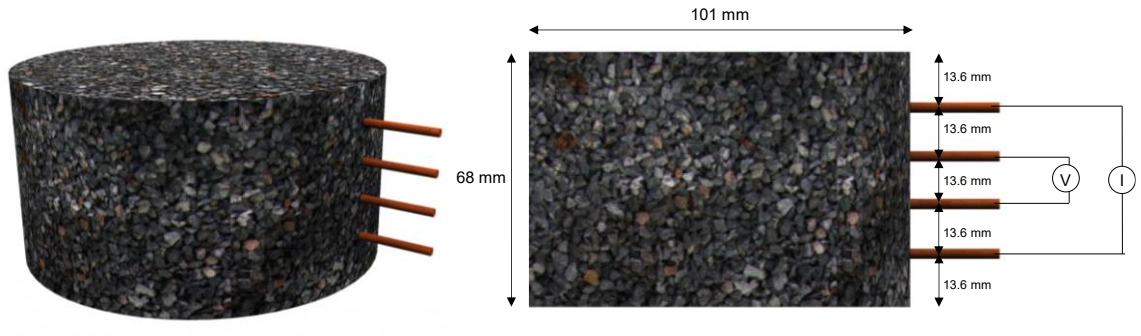

Fig. 6. Four-probe method for the electrical measurement of the asphalt mixtures

The apparent electrical resistivity ρ (Ω·m) of the asphalt mixtures is then estimated through the Wenner array method [35,43]:

$$\rho = 2 \cdot \pi \cdot s \cdot R \tag{5}$$

Where s (m) is the distance between the electrodes and R (Ω) is the electrical resistance. Chung [46] reported that the electrical resistivity measurement could reflect the degree of dispersion of the conductive particles inside the mixture. For this reason, in the present research, the standard deviation of the electrical resistivity among the different specimens was used as an indicator of the quality of GNPs dispersion within the asphalt mixture.

3.3. Self-sensing measurement

The self-sensing assessment of conductive asphalt mixtures consisted of subjecting the specimens to different kinds of compressive stress tests and simultaneously measuring the corresponding fractional change in the electrical resistance (FCR), as described in Eq.1. The compression test was widely used to assess the piezoresistive properties of asphalt mixtures and other composites materials [35,47,48].

The compressive stress was applied with a UCS loading machine (Wykeham Farrance 50 kN), while the electrical measurement was conducted according to the procedure described in Section 3.2. Both electrical and mechanical data were recorded with a frequency of 1.25 Hz. The experimental setup is shown in Fig. 7. Load and electrical data were recorded with two separate PC and then synchronized.

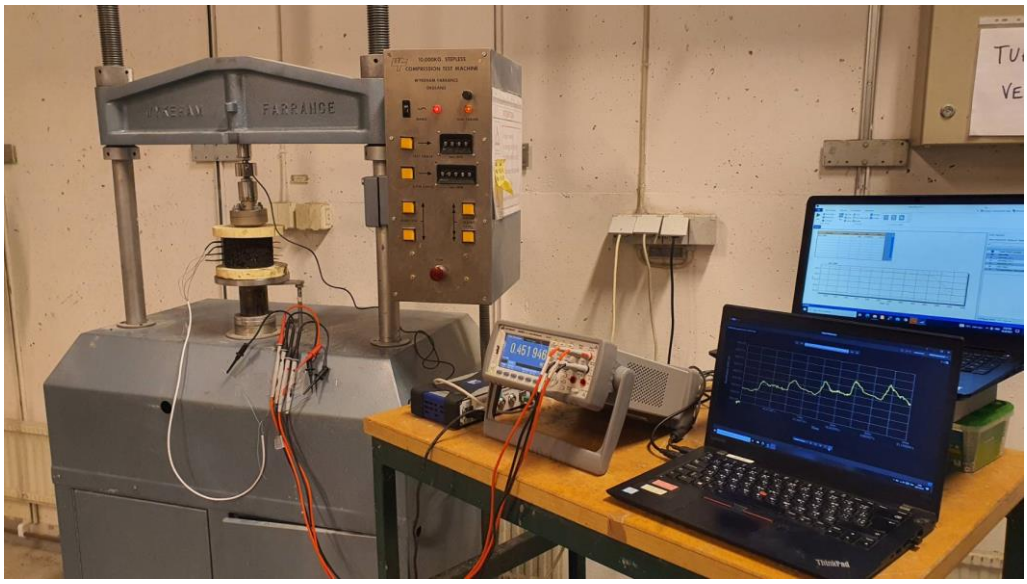

Fig. 7. Experimental setup for the piezoresistive measurement

The self-sensing properties were firstly estimated with a series of uniaxial cyclic compression tests at various load amplitudes. The objective was to assess the capability of the conductive asphalt mixture to detect the traffic flow. Different stress amplitudes were used to verify the possibility of detecting different vehicle categories (cars, trucks, etc.). The piezoresistive response was evaluated at four stress amplitudes: 0.06, 0.2, 0.4, and 0.6 MPa. The selection of this range of stress amplitudes is coherent with the stresses induced by different types of vehicles on the asphalt pavement. The loading rate was set to 1 mm/min. All the specimens were subjected to three loading cycles for each stress amplitude. Three specimens for each type of mixture were tested to determine data reproducibility.

Piezoresistive response of EAFS+GNPs asphalt mixtures was further assessed with a uniaxial compression test until the failure of the specimen, at a loading rate of 0.5 mm/min. FCR was simultaneously measured during the uniaxial compression test to assess the piezoresistive response. The objective of the test was to simulate the deterioration process of the pavement and evaluate the ability of EAFS+GNPs asphalt mixture to sense the damage evolution for SHM applications. To do this, the fractional change in resistance was assessed as a function of the percentage of breaking load, C, in %:

$$C\ (\%) = \frac{F}{F_{max}} \cdot 100 \tag{6}$$

Where F is the load and F_{max} is the ultimate load before the failure of the specimen. At the beginning of the compression test, C is equal to 0%. As the test progresses, the specimen starts to deteriorate, until its complete failure, when the percentage of breaking load C reaches 100%. It is expected that the self-sensing mixture has the ability to sense the gradual deterioration of the specimen during the test. Therefore, a gradual increase in the FCR during the test would be an indicator of the effectiveness of the self-sensing response. Three specimens for each type of mixture were tested to check data reproducibility.

3.4. Data smoothing

The acquired electrical data are inevitably affected by measurement noise. Therefore, a signal processing procedure is required to remove the noise and obtain effective sensing information

[20]. To reduce noise, Savitzky–Golay smoothing filter was used [49]. The Savitzky–Golay (SG) filter is a digital filter applied to a series of equally spaced data points. In general, digital filters aim at replacing each data value f_i by a linear combination g_i of itself and some number of surrounding data:

$$g_i = \sum_{n=-n_L}^{n_R} c_n \cdot f_{i+n} \quad (7)$$

Where n_L and n_R are the numbers of data points to the left and to the right, respectively, and c_n represent a series of filter coefficients. The number $n_L + n_R + 1$ is known as the window size *w*. For each data point f_i, SG filter is obtained by least-square fitting a polynomial of degree *d* to all $n_L + n_R + 1$ points and then set g_i to be the value of that polynomial at position *i* [50].

Two parameters should be tuned to apply the SG filter: the polynomial degree, *d*, and the window size, *w*. The present research used the trial and error method to fit the parameters. This means that various values of both *d* and *w* were tested, and the smoothing performance was graphically evaluated. Python programming language was employed for the smoothing analysis, using the Savitzky–Golay filter function already implemented into the SciPy library.

4. Results

4.1. Volumetric and mechanical performance

The volumetric properties of the asphalt mixtures are shown in Figs. 8 and 9. Each value represents the average of three specimens, and the error bars represent the standard deviations.

The bulk density was equal to 2.30, 2.55, 2.53, 2.51 and 2.48 g/cm^3 for Reference, EAFS, EAFS+GNPs-3%, EAFS+GNPs-5% and EAFS+GNPs-7% mixtures, respectively. It can be observed that mixtures with EAFS had higher bulk density than the Reference mixture. This is due to the higher specific gravity of EAFS when compared with porphyry aggregates, which cause an increase in the overall bulk density of the mixtures. By increasing the GNPs content, the bulk density of the mixture decreased. Although GNPs were added in relatively low content, 3%, 5%, and 7% by weight of the binder, they occupy a large volume inside the specimen, due to the low density of GNPs. As a result, the increase in the volume of the specimens is not balanced with an equivalent increase in the weight, leading to a reduction in the bulk density of the asphalt mixture. The results of the present study are coherent with those obtained by other authors with similar additives (i.e., graphite) on various composite materials [51,52].

As shown in Fig. 9, Reference and EAFS mixtures had similar average air voids content, 6.47 and 6.55, respectively. Both mixtures had the same grading curve (see Table 1). However, as indicated in Section 2.1, the bitumen content in the Reference mixture was lower (5% by weight of the mixture) than EAFS mixture (5.7%), to take into account the higher porosity of EAFS aggregates. This result is coherent with those of other authors [40,41], which suggest using higher bitumen content for EAFS mixtures. GNPs had the effect of reducing the air voids content of the asphalt mixture. EAFS+GNPs-3%, EAFS+GNPs-5% and EAFS+GNPs-7% mixtures had an average air voids content of 5.1, 4.0, and 3.2 %, respectively. This was probably due to the small size of GNPs, which allows the particles to fill the air voids inside the asphalt mixture.

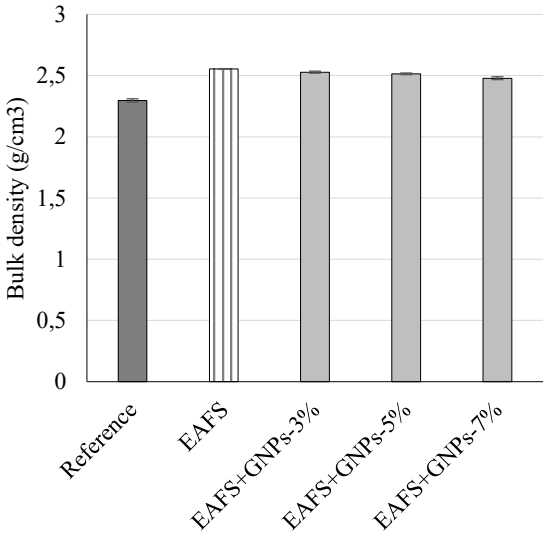

Fig. 8. Bulk density of the asphalt mixtures

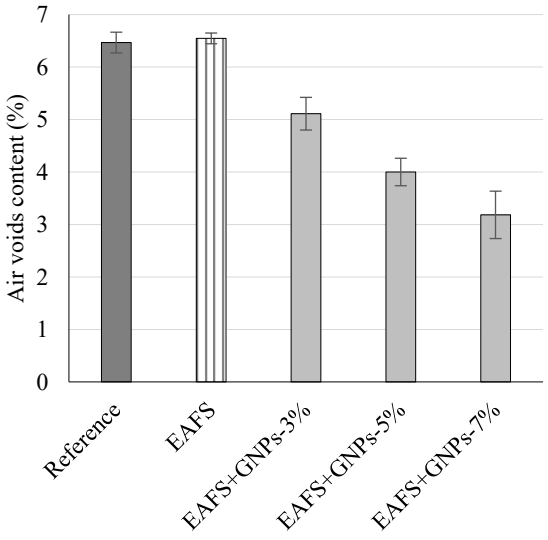

Fig. 9. Air voids content of the asphalt mixtures

Figs. 10 and 11 report the results of the Indirect tensile stiffness modulus (ITSM) and the Indirect tensile strength (ITS) test of the asphalt mixtures. Each value represents the average of three specimens, and the error bars represent the standard deviations.

The average ITSM of Reference, EAFS, EAFS+GNPs-3%, EAFS+GNPs-5% and EAFS+GNPs-7% mixtures were equal to 2356, 2309, 2601, 2536 and 2536 MPa. It can be observed that the mixtures with GNPs had slightly higher ITSM than the other mixtures, which is in line with the results of other authors [53] and revealed that the addition of GNPs does not compromise the stiffness of the mixture. However, no significant differences were observed between mixtures with different content of GNPs.

The average ITS of Reference, EAFS, EAFS+GNPs-3%, EAFS+GNPs-5%, and EAFS+GNPs-7% mixtures were equal to 1.599, 1.576, 1.539, 1.444, 1.474 MPa, respectively, showing a slightly decreasing trend with the addition of GNPs. However, it must be highlighted that the values obtained for the mixtures with GNPs are coherent with those obtained by other authors with

conventional asphalt mixtures [54,55], proving that the incorporation of GNPs up to 7% does not compromise the mechanical performance of road pavement, in terms of ITS.

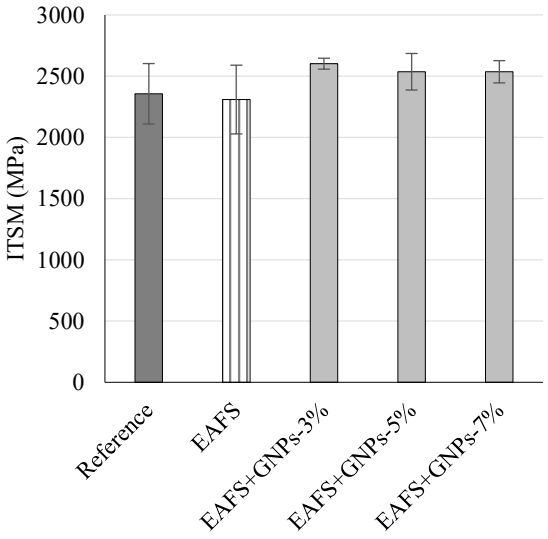

Fig. 10. ITSM of the asphalt mixtures

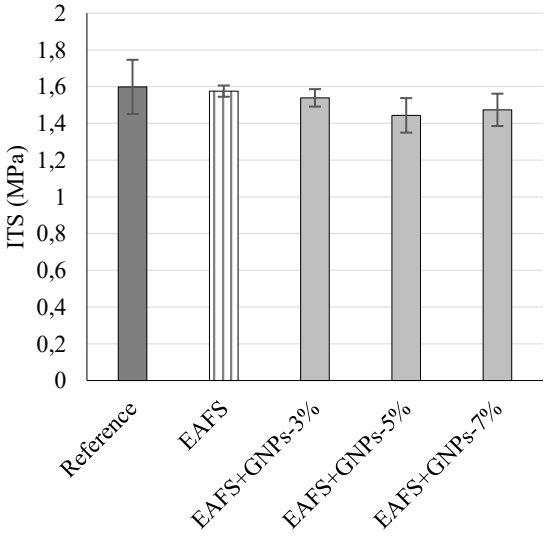

Fig. 11. ITS of the asphalt mixtures

4.2. Electrical resistivity of EAFS+GNPs asphalt mixtures

The addition of GNPs had the effect of reducing the apparent resistivity of the asphalt mixtures, Fig. 12. Each value represents the average of three specimens, and the error bars represent the standard deviations.

The average electrical resistivity of the mixtures was $2.4 \cdot 10^4$, $1.7 \cdot 10^{4,}$ and $4.1 \cdot 10^2$ Ω·m for EAFS+GNPs-3%, EAFS+GNPs-5% and EAFS+GNPs-7% mixtures, respectively. Although the difference between the mixtures with 3% and 5% is relatively low, a further increase of GNPs content of 7% caused an abrupt decrease of approximately 98% in the electrical resistivity,

probably due to the percolation phenomena [22]. Therefore, the addition of 7% of GNPs showed the best performance in enhancing the electrical conductivity of the tested asphalt mixture.

The standard deviations of the electrical resistivity of the asphalt mixture can give an indication of the dispersion performance of GNPs inside the asphalt mixture. For each mixture, it can be observed that the standard deviations were equal to 3901, 6735, and 69 Ω·m for EAFS+GNPs-3%, EAFS+GNPs-5% and EAFS+GNPs-7% mixtures, respectively. Considering the order of magnitude of the electrical resistivity values, which reach values $2.4 \cdot 10^4$, the obtained standards deviations are very low, meaning that a uniform dispersion of the GNPs among the three specimens was obtained.

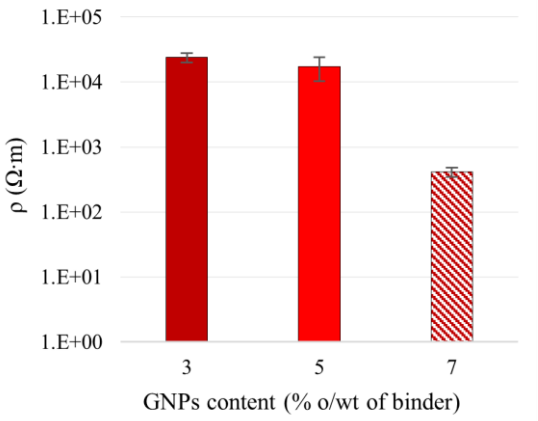

Fig. 12. Effect of GNPs on the electrical resistivity

4.3. Savitzky–Golay smoothing performance

Fig. 13 shows the effect of the window length (w) and the polynomial degree (d) on the Savitzky–Golay SG smoothing performance. For a window length equal to $w = 5$ (Fig. 13a), it can be observed that the smoothing is not effective, as the resulting curve follows almost perfectly the raw data, leading to overfitting problems. By increasing the window length, the smoothing effectiveness increased. However, if the value of w is too high ($w = 85$) (Fig. 13c), the smoothing curve cannot preserve the original shape of the data. This can lead to underestimating the sensing properties of the mixture, as the peaks of the smoothed curve are lower than the raw data. Using a window length of w=45 (Fig. 13b) seems to provide the best smoothing performance, as the smoothing is quite effective, and the shape of the data is preserved.

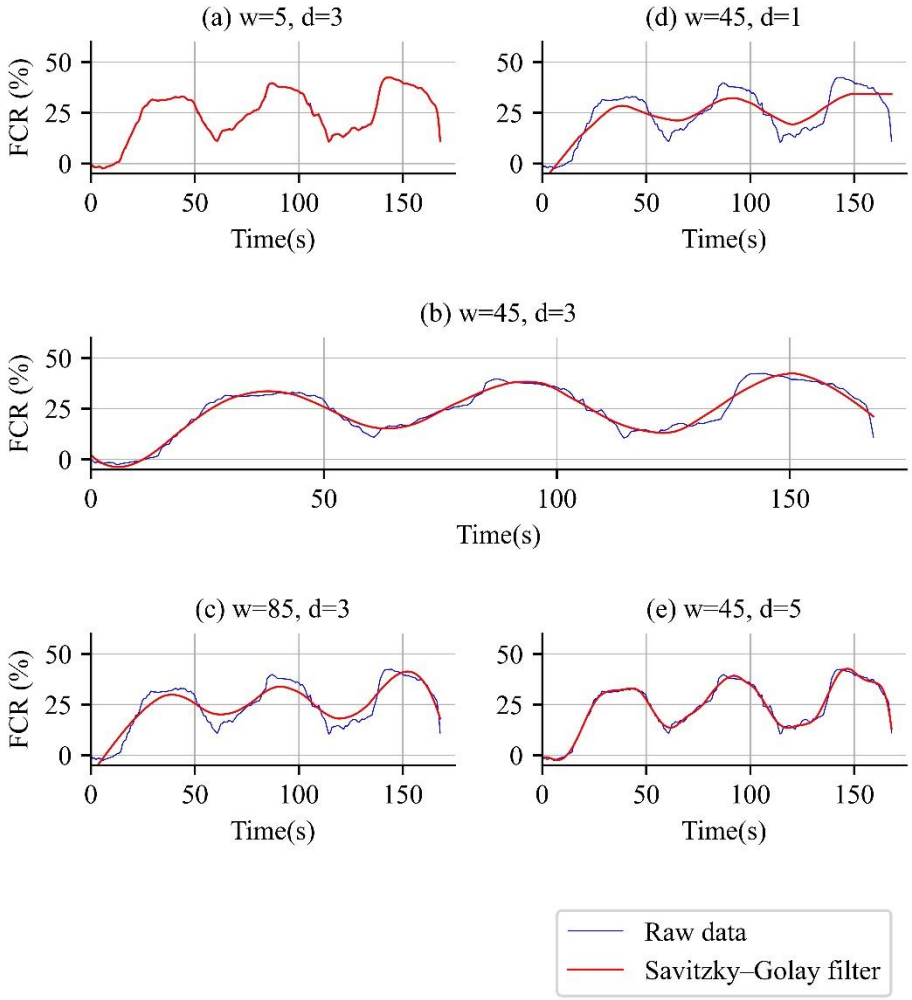

Fig. 13. Effect of the window length w and polynomial degree d on the SG smoothing performance.

On the other hand, the polynomial degree *d* produces the opposite effect. The curve is too smoothed if d is too low (d=1) (Fig. 13d). By excessively increasing the polynomial degree (*d*=5) (Fig. 13e), the smoothing performance is not effective. It can be observed that a polynomial degree of *d*=3 (Fig. 13b) provides the best smoothing results.

Therefore, Savitzky–Golay filter with a window length of *w = 45* and polynomial degree of *d*=3 was applied to all the electrical data in this research.

4.4. Piezoresistive response under uniaxial cyclic compression

The piezoresistive response of EAFS+GNPs asphalt mixtures under cyclic compression stress is shown in Figs. 14, 15, and 16. Each curve represents the average electrical response of three specimens.

For each type of mixture, it can be observed that the FCR can effectively mimic the stress state of the material, ensuring excellent self-sensing properties.

In addition, the piezoresistive response of EAFS+GNPs asphalt mixtures increased with the stress amplitudes, and this occurred for all the mixtures. For example, EAFS+GNPs-7% specimens subjected to stress amplitude of 0.06 MPa showed a FCR of approximately 2%. Increasing the

stress up to 0.2 MPa, the FCR in each cycle is almost 20%. Finally, compressing the mixture up to 0.4 and 0.6 MPa, a piezoresistive response of approximately 40% and 50% is obtained. The same considerations can be made for EAFS+GNPs-3% and EAFS+GNPs-5% mixtures. Although these mixtures can effectively sense the stress state, their piezoresistive response is lower when compared with EAFS+GNPs-7% asphalt mixtures. For compressive stress of 0.6 MPa, the FCR during loading/unloading cycles is approximately 4%, 10%, and 50% for EAFS+GNPs-3%, EAFS+GNPs-5% and EAFS+GNPs-7% mixtures, showing the superior self-sensing performance EAFS+GNPs-7% mixtures.

The previous results showed that this kind of mixture can effectively sense and distinguish different stress amplitudes. This is a very promising result for the development of a traffic detection system based on self-sensing pavements, as it would permit not only to detect the passage of the vehicles but also to identify different categories (cars, trucks, etc.).

The electrical response during repeated cyclic tests allows investigating the piezoresistive mechanism of conductive asphalt mixture. When low stress is applied (0.06 MPa) (Figs. 14a and 15a) to EAFS+GNPs-3% and EAFS+GNPs-5% mixtures, it can be observed that the FCR decreases during loading and increase during unloading, showing a positive piezoresistive effect (Fig. 2). In accordance with the piezoresistive mechanism proposed by Wu et al. [8], this can be explained by the fact that, under compression, the conductive particles tend to approach each other, promoting the formation of new conductive paths and increasing the tunneling effect. The process is totally reversible during unloading, as the particles come back to their original position.

On the other hand, EAFS+GNPs-7% mixtures showed the opposite trend, and FCR increased during loading and decreased during unloading, showing a negative piezoresistive effect (Fig. 2). In accordance with Wu et al.[36] this behavior is mainly caused by the formation of microcracks inside the mixture and the dislocation of conductive paths. In the EAFS+GNPs-7% mixtures, the conductive particles are close together, even before applying load. As a result, the applied compressive stress cannot further enhance the conductivity. On the contrary, the formation of microcracks causes the cut of some conductive paths, increasing the electrical resistance. In the mixture with 3% and 5%, the particles were too far to sense the microcracks formation. This phenomenon can be further observed in the unloading phase of EAFS+GNPs-7% mixtures, in which the initial electrical resistance was not totally recovered because some microdamage inside the mixture was not recovered.

When higher stress is applied, from 0.2 to 0.6 MPa, all the mixtures showed a negative piezoresistive effect. This means that at these stress levels, the piezoresistive response was not due to the enhancement of contact conduction or tunneling effect but to the formation of microcracks inside the mixture, which cut the conductive network.

Furthermore, in Figs. 14, 15, and 16, it can be observed that the loading peaks are not totally in phase with the electrical peaks. Asphalt mixtures are viscoelastic materials, meaning that there exists a phase lag between the applied stress and the strain of the material. The study results suggest that the FCR of asphalt mixtures subjected to compressive stress is highly correlated with the strain response of the materials. Although strain measurement has not been realized in the present study, the relationship between strain and FCR should be assessed in future research.

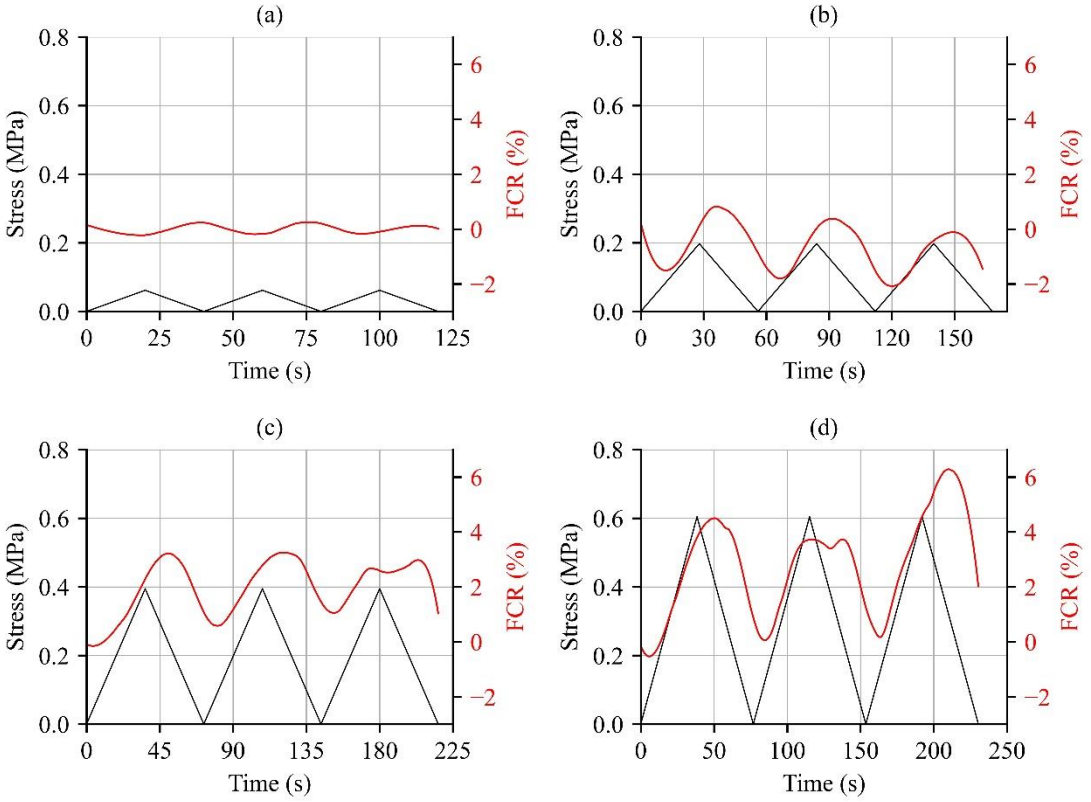

Fig. 14. Piezoresistive response of EAFS+GNPs-3% asphalt mixtures under cyclic compression stress.

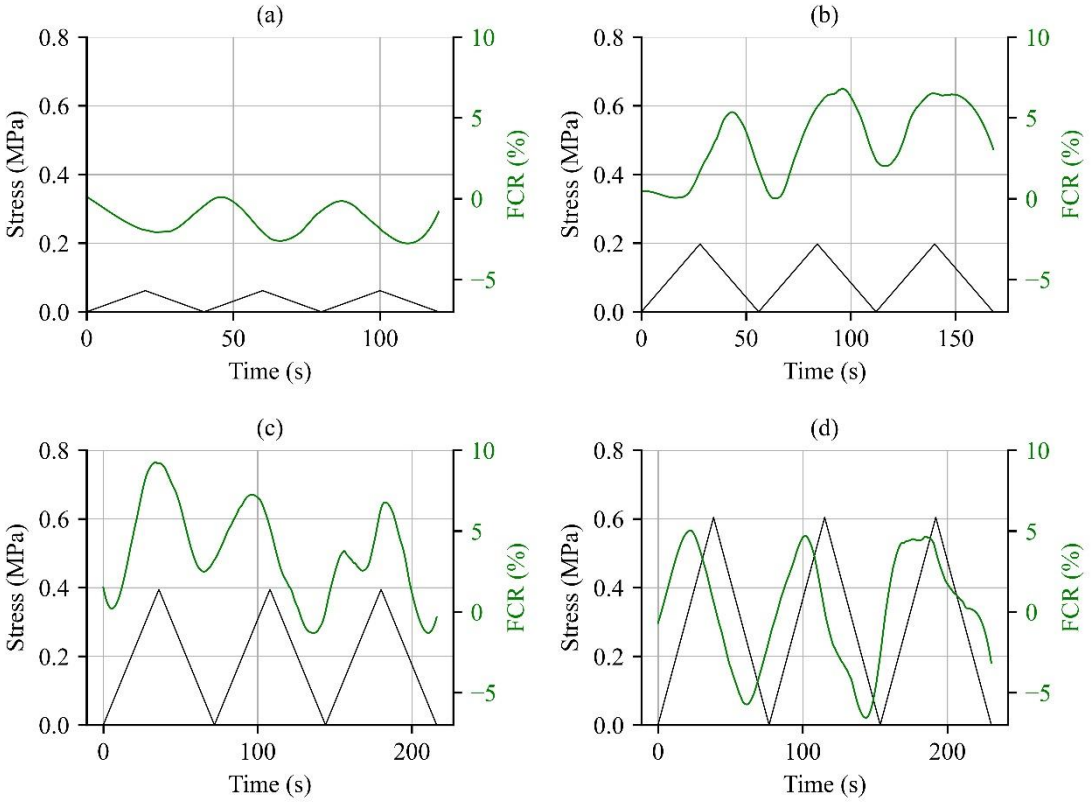

Fig. 15. Piezoresistive response of EAFS+GNPs-5% asphalt mixtures under cyclic compression stress.

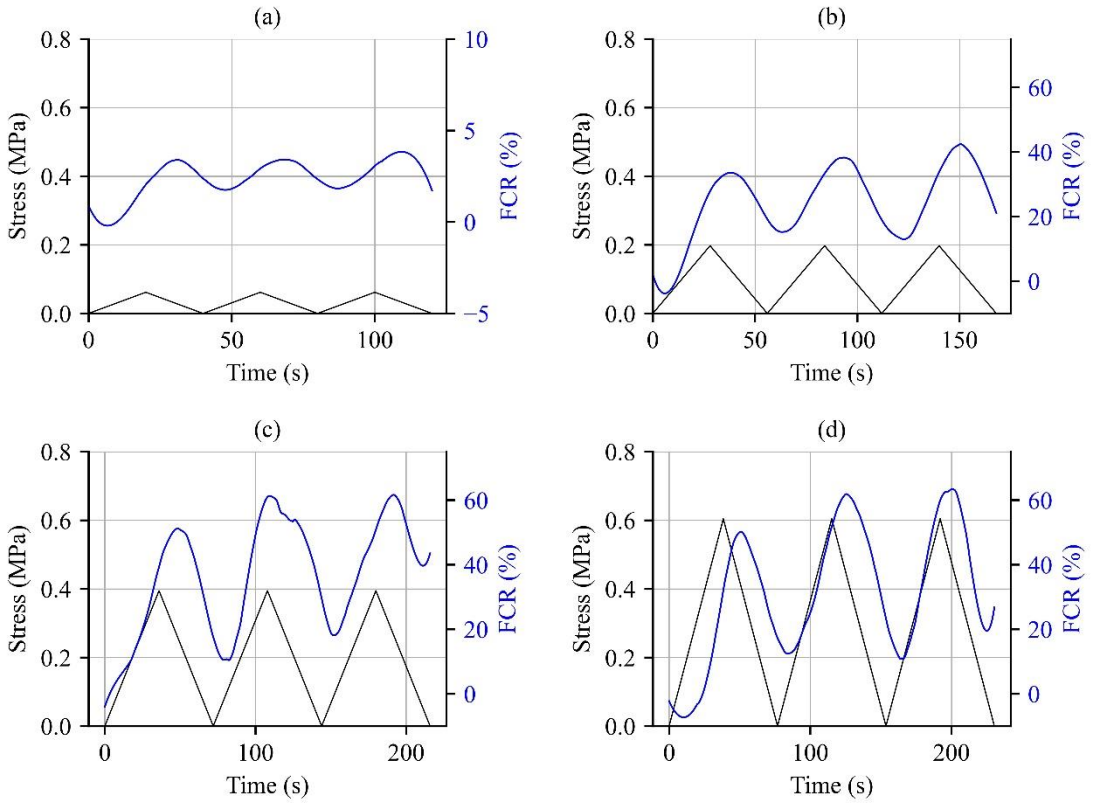

Fig. 16. Piezoresistive response of EAFS+GNPs-7% asphalt mixtures under cyclic compression stress.

4.5. Piezoresistive response under uniaxial compression until failure

Piezoresistive response of EAFS+GNPs asphalt mixtures under compression stress until the failure of the specimens is shown in Fig. 17. In each subfigure, the electrical response of three specimens is shown.

EAFS+GNPs-3% asphalt mixture specimens showed poor self-sensing properties. In the first stage of the test, the electrical resistance remained almost constant. At some point, an abrupt increase in the resistance is observed, probably due to the crack's formation. Furthermore, the abrupt jump in the FCR was observed at different moments during the test for each specimen. The jump was observed at 40%, 55%, and 85% of the percentage of breaking load, indicating that the electrical response cannot effectively predict the evolution of the deterioration of the pavement. Although this behavior is consistent with that of previous research [8,10], it does not allow the development of an efficient SHM based on the piezoresistive effect (see Fig. 3). It was reported in Section 1 that the piezoresistive effect is due to the combination of different mechanisms, such as the proximity effect (due to tunneling distance) and microcracks formation. In EAFS+GNPs-3% mixtures, the conductive network is not extensive, and the distance between GNPs particles is high. Although applying an external load can reduce the tunneling distance, the reduction in the electrical resistance is minimal as some GNPs particles are too far from each other. On the other hand, microcrack formation leads to an increase in the electrical resistance, and the resulting effect is an equilibrium state.

Increasing the load, the tunneling distance has no effect on the electrical resistance, while the microcrack mechanism seems to dominate the piezoresistive response. The few conductive paths present in the specimen are cut, and the electrical resistance is abruptly increased.

EAFS+GNPs-5% specimens showed bad sensing properties. No predictable trends were observed, and the FCR remained almost unchanged during the entire test. EAFS+GNPs-5% mixtures have a more extensive conductive network than EAFS+GNPs-3% mixtures. As a result, the distance between the conductive particles is lower, and the tunneling seems to affect the electrical resistance during all the tests. As load increases, the tunneling distance is reduced, resulting in a reduction of the electrical resistance. Simultaneously, crack formation and propagation cut some conductive paths, and the general effect is an equilibrium state for the entire test.

On the other hand, EAFS+GNPs-7% mixtures showed excellent sensing properties. For the three specimens, the FCR slightly increased during the first part of the compression test. At approximately 60% of the ultimate compression strength, the resistance started to increase more quickly. In the last stage of the test, between 90 and 100% of the percentage of breaking load, an abrupt increase in the resistance indicated the failure of the mixture. The excellent sensing performance of these specimens showing the gradual increase in the FCR, would permit to predict in real-time the deterioration state of the pavement (see Fig. 3). In addition, the absolute FCR of EAFS+GNPs-7% asphalt mixtures was significantly higher (approximately 15000 near the failure of the specimens) than for the other mixtures, further confirming its good self-sensing properties. In EAFS+GNPs-7% mixtures, it seems that conductive paths are saturated. Although some reductions in the tunneling distance can be obtained under loading, contact conduction is the primary mechanism. On the other hand, the extensive conductive network is very sensitive to the formation and generation of microcracks, leading to a gradual increase in the electrical resistance during the test.

Despite the good sensing properties of EAFS+GNPs-7% mixtures, a certain degree of variability is observed between the specimens. This can be due to several factors, such as the variability in the internal structure of the mixtures, dispersion of GNPs particles, the position of the electrodes, measurement errors, etc. Therefore, future investigations are necessary to assess the statistical uncertainty of piezoresistive measurements by analyzing different kinds of mixtures, innovative dispersion, and electrode embedment techniques.

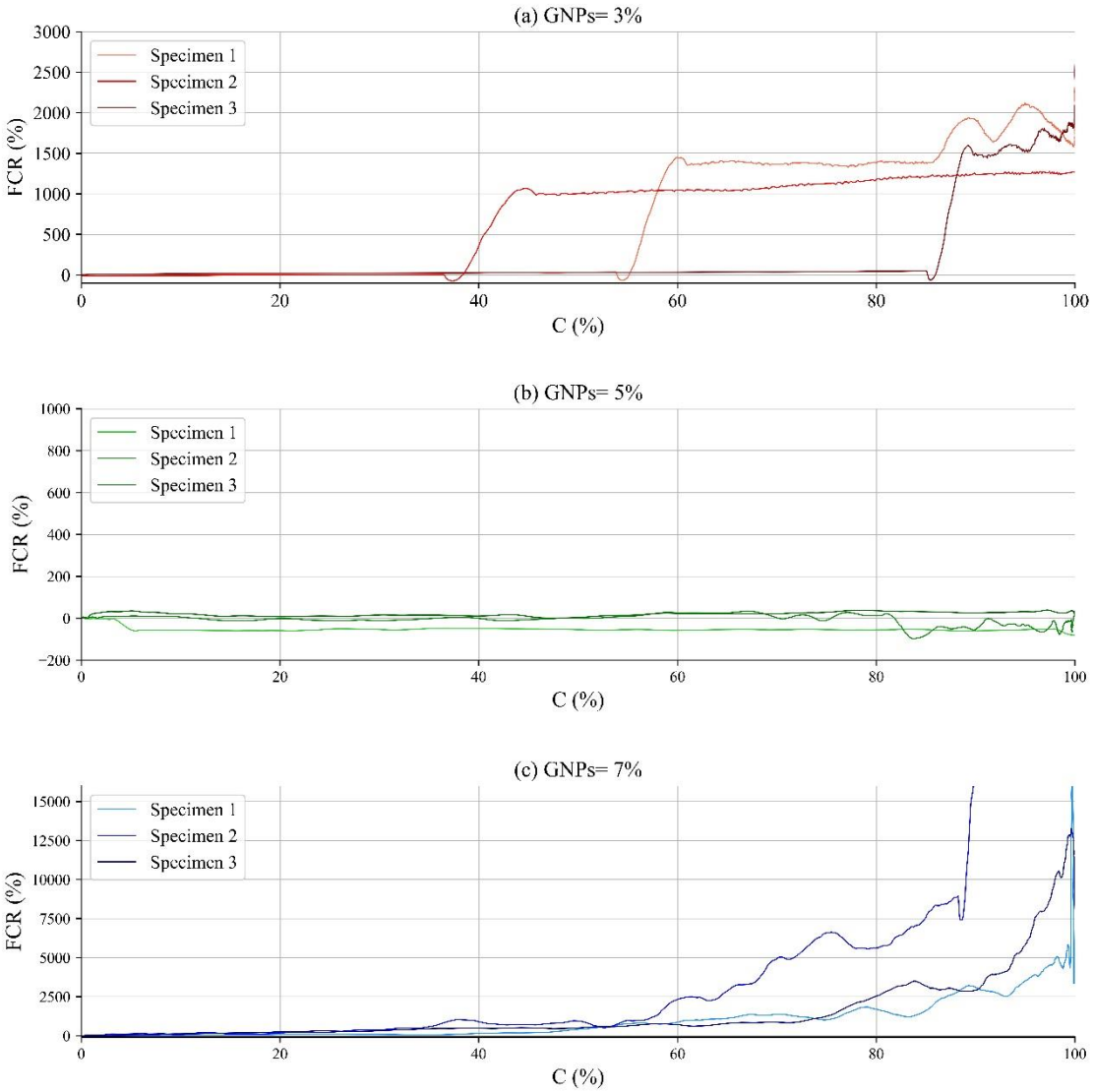

Fig. 17. Piezoresistive response of EAFS+GNPs-3%, EAFS+GNPs-5% and EAFS+GNPs-7% asphalt mixtures under compression stress until failure.

5. Conclusions

The objective of this paper was to assess the piezoresistive response of conductive stone mastic asphalt (SMA) mixtures containing electric arc furnace slag (EAFS) and graphene nanoplatelets (GNPs) for self-sensing applications. EAFS was used as fine aggregate and filler. The GNPs were added in different amounts, 3%,5%, and 7%, by weight of the binder. Different laboratory tests were made to characterize the basic properties of the asphalt mixture and assess its piezoresistive response. The following main conclusions can be drawn:

- The addition of EAFS and GNPs can effectively enhance the electrical conductivity of the asphalt mixture. EAFS+GNPs-7% asphalt mixtures showed the lowest electrical resistivity.

- GNPs decrease the bulk density and the air voids of the mixture. On the other hand, the addition of EAFS and GNPs seems to not compromise the mechanical performance of asphalt mixtures, and minor effects on the ITSM and ITS were observed.

- All the conductive asphalt mixtures, EAFS+GNPs-3%, EAFS+GNPs-5% and EAFS+GNPs-7%, can effectively mimic the stress state of the material during the cyclic loading test, providing good self-sensing properties. EAFS+GNPs-7% mixtures showed superior self-sensing properties compared with EAFS+GNPs-3% and EAFS+GNPs-5%.

- EAFS+GNPs-7% asphalt mixtures showed the ability to self-sensing their deterioration state during uniaxial compression tests performed until failure. On the contrary, EAFS+GNPs-3% and EAFS+GNPs-5% asphalt mixtures did not exhibit good sensing performance during this kind of test.

- At low stress, GNPs content seemed to influence the piezoresistive mechanism. In EAFS+GNPs-3% and EAFS+GNPs-5% mixtures, the proximity effect seemed to be the predominant mechanism, leading to a positive piezoresistivity (resistance decreases with loading). On the other hand, EAFS+GNPs-7% mixtures showed a negative piezoresistivity (resistance decreases with loading), meaning that microcracks formation could be the predominant mechanism.

- At high stress, the microcracks formation was the main factor responsible for the piezoresistive effect of all tested mixtures, leading to the recorded negative piezoresistivity.

The results of the present research can be considered as a starting point toward the development of automatic traffic detection and SHM systems based on self-sensing asphalt pavements. However, although the findings are promising, further research on this topic is needed, and some limitations of the study must be recognized.

First, asphalt pavements in service are subjected to repeated bending loads; thus, compression and tension stress exist in the road structure. Therefore, to ensure the scalability of self-sensing technology, it would be crucial to prove its effectiveness in each stress/strain condition. Second, although the stress levels induced in the specimens were consistent with those transmitted to the pavement by the traffic loads, the loading mode used in the present research is far from those that vehicles actually transfer to the pavement.

To overcome these limitations, the piezoresistive response under tension or bending tests should be evaluated in future research. In addition, more realistic loading modes, such as haversine or sinusoidal loading, should also be applied. Similarly, fatigue tests should be performed in future investigations to verify the self-sensing properties during a more realistic deterioration mechanism.

Further research is also necessary to confirm the piezoresistive behavior of asphalt mixtures and to investigate other factors affecting the self-sensing properties, such as effects of the electrodes' arrangement, environmental conditions (e.g., temperature and humidity), the volumetric and mechanical properties of the mixture and the use of different conductive additives.

Lastly, the effect of EAFS and GNPs on other mechanical performance, such as fatigue, moisture sensitivity, and rutting resistance, should be assessed.

Acknowledgements

This study has been financed by the research project Sensing PAVE (PID2020-118987RB-I00) of the Spanish Ministry of Science and Innovation and by UPM (Universidad Politécnica de Madrid) Programa Propio 2021 "Ayudas al personal investigador en formación predoctoral

contratado o becado OTT para realizar una estancia de investigación internacional para la obtención de la mención internacional de doctorado".

References

[1] F. Chen, N. Taylor, R. Balieu, N. Kringos, Dynamic application of the Inductive Power Transfer (IPT) systems in an electrified road: Dielectric power loss due to pavement materials, Construction and Building Materials. 147 (2017) 9–16. https://doi.org/10.1016/j.conbuildmat.2017.04.149.

[2] H. Roshani, S. Dessouky, A. Montoya, A.T. Papagiannakis, Energy harvesting from asphalt pavement roadways vehicle-induced stresses: A feasibility study, Applied Energy. 182 (2016) 210–218. https://doi.org/10.1016/j.apenergy.2016.08.116.

[3] D. Sun, G. Sun, X. Zhu, A. Guarin, B. Li, Z. Dai, J. Ling, A comprehensive review on self-healing of asphalt materials: Mechanism, model, characterization and enhancement, Advances in Colloid and Interface Science. 256 (2018) 65–93. https://doi.org/10.1016/J.CIS.2018.05.003.

[4] J. Gallego, F. Gulisano, V. Contreras, A. Páez, The crucial effect of re-compaction energy on the healing response of hot asphalt mortars heated by microwaves, Construction and Building Materials. 285 (2021) 122861. https://doi.org/10.1016/j.conbuildmat.2021.122861.

[5] M. Abedi, R. Fangueiro, A. Gomes Correia, A review of intrinsic self-sensing cementitious composites and prospects for their application in transport infrastructures, Construction and Building Materials. 310 (2021) 125139. https://doi.org/10.1016/j.conbuildmat.2021.125139.

[6] J. Zhang, Y. Lu, Z. Lu, C. Liu, G. Sun, Z. Li, A new smart traffic monitoring method using embedded cement-based piezoelectric sensors, Smart Materials and Structures. 24 (2015) 025023. https://doi.org/10.1088/0964-1726/24/2/025023.

[7] J. Nedoma, M. Fajkus, R. Martinek, J. Vanus, S. Kepak, R. Kahankova, R. Jaros, D. Cvejn, M. Prauzek, Analysis of the use of fiber-optic sensors in the road traffic, in: IFAC-PapersOnLine, Elsevier B.V., 2018: pp. 420–425. https://doi.org/10.1016/j.ifacol.2018.07.117.

[8] S. Wu, X. Liu, Q. Ye, N. Li, Self-monitoring electrically conductive asphalt-based composite containing carbon fillers, Transactions of Nonferrous Metals Society of China. 16 (2006) s512–s516. https://doi.org/10.1016/s1003-6326(06)60246-x.

[9] D.D.L. Chung, Multifunctional cement-based materials, M. Dekker, 2003, ISBN: 9780824746100.

[10] X. Liu, S. Wu, Research on the conductive asphalt concrete's piezoresistivity effect and its mechanism, Construction and Building Materials. 23 (2009) 2752–2756. https://doi.org/10.1016/j.conbuildmat.2009.03.006.

[11] X. Liu, S. Wu, N. Li, B. Gao, Self-monitoring application of asphalt concrete containing graphite and carbon fibers, Journal Wuhan University of Technology, Materials Science Edition. 23 (2007) 268–271. https://doi.org/10.1007/s11595-006-2268-2.

[12] A. Zhang, K.C.P. Wang, B. Li, E. Yang, X. Dai, Y. Peng, Y. Fei, Y. Liu, J.Q. Li, C. Chen, Automated Pixel-Level Pavement Crack Detection on 3D Asphalt Surfaces Using a Deep-Learning Network, Computer-Aided Civil and Infrastructure Engineering. 32 (2017) 805–819. https://doi.org/10.1111/mice.12297.

[13] Z. Tong, J. Gao, A. Sha, L. Hu, S. Li, Convolutional Neural Network for Asphalt Pavement Surface Texture Analysis, Computer-Aided Civil and Infrastructure

Engineering. 33 (2018) 1056–1072. https://doi.org/10.1111/mice.12406.

[14] A. Karimzadeh, O. Shoghli, Predictive analytics for roadway maintenance: A review of current models, challenges, and opportunities, Civil Engineering Journal (Iran). 6 (2020) 602–625. https://doi.org/10.28991/cej-2020-03091495.

[15] B. Han, X. Yu, E. Kwon, A self-sensing carbon nanotube/cement composite for traffic monitoring, Nanotechnology. 20 (2009) 445501. https://doi.org/10.1088/0957-4484/20/44/445501.

[16] B. Han, K. Zhang, X. Yu, E. Kwon, J. Ou, Nickel particle-based self-sensing pavement for vehicle detection, Measurement: Journal of the International Measurement Confederation. 44 (2011) 1645–1650. https://doi.org/10.1016/j.measurement.2011.06.014.

[17] Z.Q. Shi, D.D.L. Chung, Carbon fiber-reinforced concrete for traffic monitoring and weighing in motion, Cement and Concrete Research. 29 (1999) 435–439. https://doi.org/10.1016/S0008-8846(98)00204-X.

[18] W. Dong, W. Li, Z. Tao, K. Wang, Piezoresistive properties of cement-based sensors: Review and perspective, Construction and Building Materials. 203 (2019) 146–163. https://doi.org/10.1016/j.conbuildmat.2019.01.081.

[19] J. Han, J. Pan, J. Cai, X. Li, A review on carbon-based self-sensing cementitious composites, Construction and Building Materials. 265 (2020) 120764. https://doi.org/10.1016/j.conbuildmat.2020.120764.

[20] B. Han, S. Ding, X. Yu, Intrinsic self-sensing concrete and structures: A review, Measurement: Journal of the International Measurement Confederation. 59 (2015) 110–128. https://doi.org/10.1016/j.measurement.2014.09.048.

[21] P. Ahmedzade, B. Sengoz, Evaluation of steel slag coarse aggregate in hot mix asphalt concrete, Journal of Hazardous Materials. 165 (2009) 300–305. https://doi.org/10.1016/j.jhazmat.2008.09.105.

[22] S. Wu, L. Mo, Z. Shui, Z. Chen, Investigation of the conductivity of asphalt concrete containing conductive fillers, Carbon. 43 (2005) 1358–1363. https://doi.org/10.1016/j.carbon.2004.12.033.

[23] I.W. Nam, H. Souri, H.K. Lee, Percolation threshold and piezoresistive response of multi-wall carbon nanotube/cement composites, Smart Structures and Systems. 18 (2016) 217–231. https://doi.org/10.12989/sss.2016.18.2.217.

[24] X. Liu, S. Wu, Q. Ye, J. Qiu, B. Li, Properties evaluation of asphalt-based composites with graphite and mine powders, Construction and Building Materials. 22 (2007) 121–126. https://doi.org/10.1016/j.conbuildmat.2006.10.004.

[25] A. Arabzadeh, H. Ceylan, S. Kim, A. Sassani, K. Gopalakrishnan, M. Mina, Electrically-conductive asphalt mastic: Temperature dependence and heating efficiency, Materials & Design. 157 (2018) 303–313. https://doi.org/10.1016/J.MATDES.2018.07.059.

[26] Á. García, E. Schlangen, M. van de Ven, Q. Liu, Electrical conductivity of asphalt mortar containing conductive fibers and fillers, Construction and Building Materials. 23 (2009) 3175–3181. https://doi.org/10.1016/J.CONBUILDMAT.2009.06.014.

[27] H. Wang, J. Yang, H. Liao, X. Chen, Electrical and mechanical properties of asphalt concrete containing conductive fibers and fillers, Construction and Building Materials. 122 (2016) 184–190. https://doi.org/10.1016/j.conbuildmat.2016.06.063.

[28] F. Gulisano, J. Crucho, J. Gallego, L. Picado-Santos, Microwave Healing Performance

of Asphalt Mixture Containing Electric Arc Furnace (EAF) Slag and Graphene Nanoplatelets (GNPs), Applied Sciences. 10 (2020) 1428. https://doi.org/10.3390/app10041428.

[29] I. Pérez, Y. Agzenal, J. Pozuelo, J. Sanz, J. Baselga, A. García, V. Pérez, Self-healing of asphalt mixes, containing conductive modified bitumen,using microwave heating, in: 6th Eurasphalt & Eurobitume Congress, 2016. https://doi.org/dx.doi.org/10.14311/EE.2016.288.

[30] J. Gallego, F. Gulisano, V. Contreras, A. Páez, Optimising heat and re-compaction energy in the thermomechanical treatment for the assisted healing of asphalt mixtures, Construction and Building Materials. 292 (2021) 123431. https://doi.org/10.1016/j.conbuildmat.2021.123431.

[31] P. Pan, S. Wu, F. Xiao, L. Pang, Y. Xiao, Conductive asphalt concrete: A review on structure design, performance, and practical applications, Journal of Intelligent Material Systems and Structures. 26 (2015) 755–769. https://doi.org/10.1177/1045389X14530594.

[32] F. Gulisano, J. Gallego, Microwave heating of asphalt paving materials: Principles, current status and next steps, Construction and Building Materials. 278 (2021) 121993. https://doi.org/10.1016/j.conbuildmat.2020.121993.

[33] J. Gao, H. Guo, X. Wang, P. Wang, Y. Wei, Z. Wang, Y. Huang, B. Yang, Microwave deicing for asphalt mixture containing steel wool fibers, Journal of Cleaner Production. 206 (2019) 1110–1122. https://doi.org/10.1016/j.jclepro.2018.09.223.

[34] Q. Liu, S. Wu, E. Schlangen, Induction heating of asphalt mastic for crack control, Construction and Building Materials. 41 (2013) 345–351. https://doi.org/10.1016/j.conbuildmat.2012.11.075.

[35] H.R. Rizvi, M.J. Khattak, M. Madani, A. Khattab, Piezoresistive response of conductive Hot Mix Asphalt mixtures modified with carbon nanofibers, Construction and Building Materials. 106 (2016) 618–631. https://doi.org/10.1016/j.conbuildmat.2015.12.187.

[36] S.P. Wu, L.T. Mo, Z.H. Shui, Piezoresistivity of Graphite Modified Asphalt-based Composites, in: Key Engineering Materials, Trans Tech Publications Ltd, 2003: pp. 391–396. https://doi.org/10.4028/www.scientific.net/kem.249.391.

[37] L. Liu, X. Zhang, L. Xu, H. Zhang, Z. Liu, Investigation on the piezoresistive response of carbon fiber-graphite modified asphalt mixtures, Construction and Building Materials. 301 (2021) 124140. https://doi.org/10.1016/j.conbuildmat.2021.124140.

[38] M. Skaf, J.M. Manso, Á. Aragón, J.A. Fuente-Alonso, V. Ortega-López, EAF slag in asphalt mixes: A brief review of its possible re-use, Resources, Conservation and Recycling. 120 (2017) 176–185. https://doi.org/10.1016/J.RESCONREC.2016.12.009.

[39] F. Gulisano, J. Gallego, L. Trigos, F.R. Apaza Apaza, Dielectric characterisation of asphalt mortars for microwave heating applications, Construction and Building Materials. 308 (2021) 125048. https://doi.org/10.1016/j.conbuildmat.2021.125048.

[40] E.A. Oluwasola, M.R. Hainin, M.M.A. Aziz, Evaluation of asphalt mixtures incorporating electric arc furnace steel slag and copper mine tailings for road construction, Transportation Geotechnics. 2 (2015) 47–55. https://doi.org/10.1016/j.trgeo.2014.09.004.

[41] M. Pasetto, N. Baldo, Mix design and performance analysis of asphalt concretes with electric arc furnace slag, Construction and Building Materials. 25 (2011) 3458–3468. https://doi.org/10.1016/j.conbuildmat.2011.03.037.

[42] A.C. Ferrari, J.C. Meyer, V. Scardaci, C. Casiraghi, M. Lazzeri, F. Mauri, S. Piscanec, D. Jiang, K.S. Novoselov, S. Roth, A.K. Geim, Raman spectrum of graphene and graphene layers, Physical Review Letters. 97 (2006) 187401. https://doi.org/10.1103/PhysRevLett.97.187401.

[43] G. Cosoli, A. Mobili, F. Tittarelli, G.M. Revel, P. Chiariotti, Electrical Resistivity and Electrical Impedance Measurement in Mortar and Concrete Elements: A Systematic Review, Applied Sciences. 10 (2020) 9152. https://doi.org/10.3390/app10249152.

[44] B. Han, X. Guan, J. Ou, Electrode design, measuring method and data acquisition system of carbon fiber cement paste piezoresistive sensors, Sensors and Actuators, A: Physical. 135 (2007) 360–369. https://doi.org/10.1016/j.sna.2006.08.003.

[45] T. Buasiri, K. Habermehl-Cwirzen, L. Krzeminski, A. Cwirzen, Piezoresistive Load Sensing and Percolation Phenomena in Portland Cement Composite Modified with In-Situ Synthesized Carbon Nanofibers, Nanomaterials. 9 (2019) 594. https://doi.org/10.3390/nano9040594.

[46] D.D.L. Chung, Dispersion of Short Fibers in Cement, Journal of Materials in Civil Engineering. 17 (2005) 379–383. https://doi.org/10.1061/(asce)0899-1561(2005)17:4(379).

[47] W. Dong, W. Li, K. Wang, Z. Luo, D. Sheng, Self-sensing capabilities of cement-based sensor with layer-distributed conductive rubber fibres, Sensors and Actuators A: Physical. 301 (2020) 111763. https://doi.org/10.1016/j.sna.2019.111763.

[48] M. Abedi, R. Fangueiro, A.G. Correia, Effects of multiscale carbon-based conductive fillers on the performances of a self-sensing cementitious geocomposite, Journal of Building Engineering. 43 (2021) 103171. https://doi.org/10.1016/j.jobe.2021.103171.

[49] A. Savitzky, M.J.E. Golay, Smoothing and Differentiation of Data by Simplified Least Squares Procedures, Analytical Chemistry. 36 (1964) 1627–1639. https://doi.org/10.1021/ac60214a047.

[50] W.H. Press, S.A. Teukolsky, Savitzky-Golay Smoothing Filters, Computers in Physics. 4 (1990) 669. https://doi.org/10.1063/1.4822961.

[51] M. Ahmad, R.N.S. Al-Dala'ien, S. Beddu, Z.B. Itam, Thermo-physical Properties of Graphite Powder and Polyethylene Modified Asphalt Concrete, Engineered Science. 17 (2022) 121–132. https://doi.org/10.30919/es8d569.

[52] P. Rovnaník, I. Kusák, P. Bayer, P. Schmid, L. Fiala, Electrical and self-sensing properties of alkali-activated slag composite with graphite filler, Materials. 12 (2019). https://doi.org/10.3390/ma12101616.

[53] M. Hafeez, N. Ahmad, M. Kamal, J. Rafi, M. Haq, Jamal, S. Zaidi, M. Nasir, Experimental Investigation into the Structural and Functional Performance of Graphene Nano-Platelet (GNP)-Doped Asphalt, Applied Sciences. 9 (2019) 686. https://doi.org/10.3390/app9040686.

[54] S. Tayfur, H. Ozen, A. Aksoy, Investigation of rutting performance of asphalt mixtures containing polymer modifiers, Construction and Building Materials. 21 (2007) 328–337. https://doi.org/10.1016/j.conbuildmat.2005.08.014.

[55] N. Mashaan, A. Chegenizadeh, H. Nikraz, Performance of PET and nano-silica modified stone mastic asphalt mixtures, Case Studies in Construction Materials. 16 (2022) e01044. https://doi.org/10.1016/j.cscm.2022.e01044.